Rate-Dependent Deformation Behavior of POSS-Filled and Plasticized Poly(vinyl chloride)

S. Y. Soong,[†] R. E. Cohen,*[,†] M. C. Boyce,*[,‡] and A. D. Mulliken[‡]

Department of Chemical Engineering, Massachusetts Institute of Technology, 77 Massachusetts Avenue, Cambridge, Massachusetts 02139, and Department of Mechanical Engineering, Massachusetts Institute of Technology, 77 Massachusetts Avenue, Cambridge, Massachusetts 02139

Received December 22, 2005; Revised Manuscript Received February 16, 2006

ABSTRACT: Polymers are known to exhibit strong rate-dependent mechanical behavior. In different temperature and/or frequency regimes, the rate sensitivities of polymers change as various primary (α) and secondary (β) molecular mobility mechanisms are accessed. The incorporation of nanoparticles into the polymer matrix can potentially alter the local molecular level structure and thus offers an opportunity to tailor the rate-dependent mechanical deformation and failure behavior of the polymer. In this study, methacryl-POSS is incorporated into poly(vinyl chloride), producing a range in weight fraction of well-dispersed POSS. Dioctyl phthalate (DOP) plasticized PVC is also prepared with a range in DOP content using the same method. Both methacryl-POSS and DOP plasticize the PVC. Dynamic mechanical analysis (DMA) revealed that the incorporation of POSS in PVC introduced reductions in both the primary (α) and secondary (β) transition temperatures. DOP reduced the α-transition temperature in the blends, whereas a pronounced suppression of the β-relaxation peak was observed at higher DOP content. The rate-dependent yield and postyield behavior are characterized in compression testing over a wide range of strain rates (10^{-4}−3000/s). A clear rate-dependent transition associated with the strain-rate-dependent relaxation of β-motions was observed in the compression yield data of PVC/POSS blends. Such a transition was much milder in the case of PVC/DOP due to the suppression of the β-transition in these blends.

1. Background

Polymers are known to exhibit strong time-dependent mechanical behavior, as evidenced by rate-dependent moduli, yield strength, postyield behavior, and failure mechanisms. Generally, the yield stress required for plastic deformation increases with decreasing temperature or increasing strain rate. A transition in the rate dependence of the yield behavior over a wide range of temperature (−50 to 150 °C) and strain rate (10^{-5}−10^{-1}/s) has been observed in various glassy polymers including poly(methyl methacrylate) (PMMA),[1,2] polycarbonate (PC),[3,4] and poly(vinyl chloride) (PVC).[3] These studies revealed that two rate processes are involved in activating inelastic deformation. As the temperature is reduced and/or the strain rate is increased, an additional stress is required to activate the secondary (β) process in order for the material to yield.

Figure 1 shows the rate-dependent yield behavior of PVC from −50 to 70 °C over a range in strain rate of 10^{-5}−10^{-1}/s.[3] Below the indicated line *d*, the molecular motions governing yield mainly correspond to the main-chain α-relaxation motions, commonly associated with the glass transition. Over the small range in temperature of the α-transition, the polymer behavior transitions from glassy to rubbery with increasing temperature. Above line *d*, the β-motions associated with local relaxation movements of small groups along the chain become important, and a nonnegligible stress is required to activate β-motions to enable yield. The intersection of each σ_y/T curve with *d* reveals the character of the frequency or rate dependence of the β-transition temperature. Recently, the rate-dependent elastic−plastic deformation of PC and PMMA was investigated by Mulliken and Boyce[5,6] over the strain rate range of 10^{-3}−3000/s; both materials exhibited increased rate sensitivity of yield under the same strain rate/temperature conditions as the β-transition.

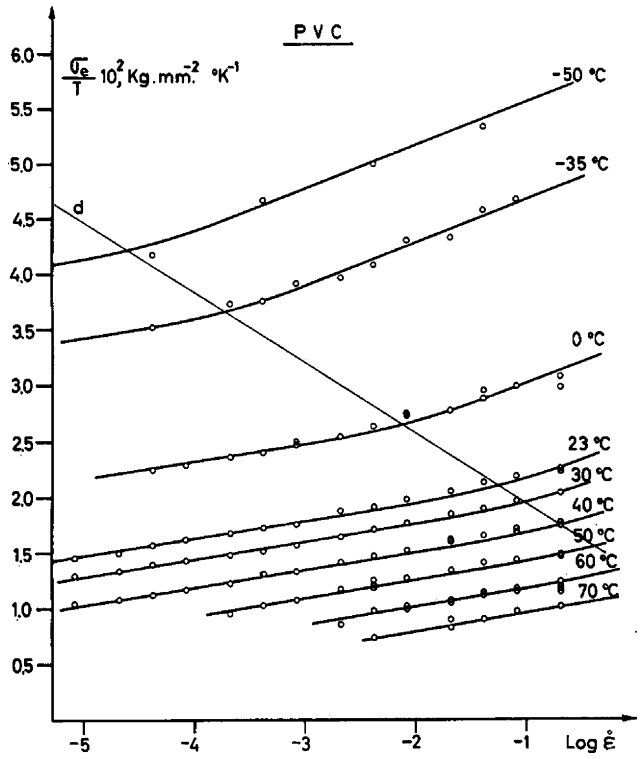

Figure 1. Yield data of poly(vinyl chloride) presented by Bauwens-Crowet et al.. The set of parallel curves was calculated from Ree−Eyring theory.[3]

As nanoparticles are incorporated into a polymer, the molecular level modifications offer opportunities to tailor the rate-dependent mechanical deformation and failure behavior of the polymer. Polymer nanocomposites have drawn much attention

* Corresponding authors: Tel +1-617-253-3777, +1-617-253-2342, e-mail:recohen@mit.edu, mcboyce@mit.edu.
[†] Department of Chemical Engineering.
[‡] Department of Mechanical Engineering.

10.1021/ma052736s CCC: $33.50 © 2006 American Chemical Society
Published on Web 03/17/2006

due to the potential for improvement in properties including modulus, strength, toughness, thermal stability, and gas permeability. Research regarding α- and β-relaxation processes of polymer nanocomposites has been conducted to understand the influence of nanoparticles on polymeric molecular motions.[7−9] Böhning et al.[7,8] showed that incorporating a low content of SiC nanoparticles in PC has no effect on the α-transition; however, the β-transition is broadened and the activation energy of the β-transition is reduced with increasing nanoparticle concentration.[7] Kuila et al. showed that the α- and β-transition temperatures and the melting point of poly(3-hexylthiophene) were increased when montmorillonite clay particles are incorporated into the polymer system and the 1% clay content polymer nanocomposite exhibits the maximum thermal stability.[9]

This study focuses on the rate-dependent deformation behavior of polymer compounds comprised of polyhedral oligomeric silsesquioxanes (POSS) blended with PVC. POSS has received much interest due to its hybrid organic−inorganic structure which consists of a silica cage with functional groups attached at the cage corners. When POSS is covalently attached to the polymer backbones, POSS has been shown to improve physical and mechanical properties, such as increased glass transition temperature (T_g),[10,11] improved thermoxidative stability,[12] and higher storage modulus at low temperature,[11] due to the reinforcement at the molecular level.[13] POSS can also be incorporated into homopolymers through direct blending. Increase in free volume and initial plasticization of the polymer matrix have been observed when untethered POSS is well-dispersed within the polymer.[14] POSS tends to aggregate within a polymer matrix (e.g., refs 15 and 14) with increasing weight fraction, and the aggregates can act like stiff fillers. Mulliken and Boyce showed that trisilanophenyl-POSS (5 wt %) has little effect on the PC α-transition region, but the POSS enhances the mobility of the β-motions significantly and therefore reduces the resistance in high rate deformation.[16] Here, the effects of various weight fractions of POSS on the elastic and plastic deformation behavior of PVC at different rates are studied and compared to that obtained when blending different weight fraction of the DOP into PVC.

2. Experiments

2.1. Materials. The poly(vinyl chloride) used in this study was custom-made by Scientific Polymer Products, Inc. (Ontario, NY) with an approximate molecular weight of 90 000 g/mol. Methacryl-POSS was obtained from Hybrid Plastics (Fountain Valley, CA). It is a noncrystallizable mixture of 8-, 10-, 12-, and 14-corner POSS cages, with 10-corner cages having the highest weight fraction (≈47 wt % as measured by NMR[17]). Methacryl-POSS appears in the form of a light brown heavy oil at room temperature. Figure 2 shows the chemical structure of a 10-corner methacryl-POSS molecule. Kopesky et al.[14] showed that cyclohexyl-POSS or isobutyl-POSS can be blended into PMMA, producing nanocomposites with excellent dispersion up to a volume fraction of 1%. At higher volume fraction, the POSS was found to aggregate and crystallize into larger particles. Since the methacryl-POSS cage mixture does not form crystallites at room temperature, a higher loading limit is expected.[17]

Neat PVC; 10, 15, and 20 wt % of methacryl-POSS in PVC; and 10, 15, and 20 wt % of dioctyl phthalate (DOP, Sigma-Aldrich) in PVC were prepared for this study. After a targeted percentage of methacryl-POSS or DOP was mixed into PVC powders, the mixture was then melt-blended for 2 min in a lab scale extruder (DACA Instruments). The PVC used in all of the polymer blends contained 3 wt % of thermal stabilizer (Thermolite 890S, Atofina) to minimize degradation.

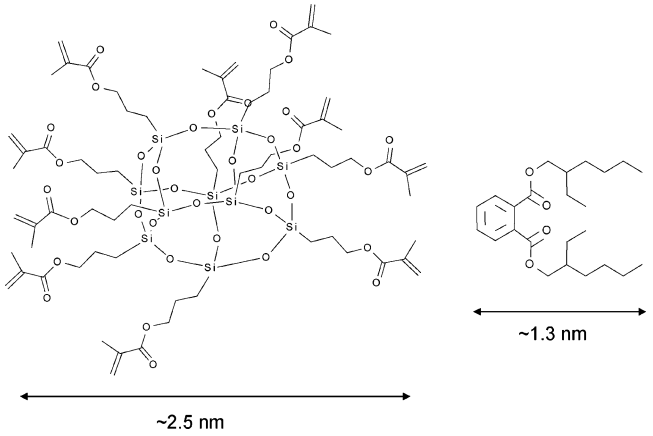

Figure 2. Molecular structures of a 10-corner cage methacryl-POSS molecule and a DOP molecule.

2.2. Dynamic Mechanical Analysis. Dynamic mechanical analysis (DMA) was performed on a TA Instruments Q800 DMA to observe and investigate the α- and β-transitions of the materials in this study. Cylindrical polymer samples with a diameter of 2.5 mm and a length of 15 mm were tested in the cantilever mode in DMA with a fixed displacement of 25 μm. The testing temperature ranged from −100 to 140 °C with a 2 °C/min heating rate at frequencies of 1, 10, and 100 Hz. The particular frequencies of these tests were converted to corresponding average strain rates, giving a range in strain rate of 5×10^{-3}−5.8×10^{-1}/s.[30] Since the storage and loss modulus are frequency-dependent, converting the frequencies to corresponding strain rates allows us to relate the DMA data to the compression testing results. The same tests were repeated three times for each blend composition using three different specimens. Storage modulus and loss modulus were measured as a function of temperature, and the corresponding tan δ was calculated.

2.3. Compression and Tensile Testing. Uniaxial compression tests were performed over a wide range of strain rates: 10^{-4}/s to nearly 3000/s. Extruded polymer strands were pelletized, compression-molded into disks, and then machined into specimens for compression testing. Low to moderate rate compression testing (10^{-4}−10^{-1}/s) was accomplished on a Zwick mechanical tester (Zwick Roell Group). All specimens were machined to right circular cylinders with diameter of 9 mm and height of 4.5 mm. To reduce friction, thin Teflon films were placed between specimen and compression platens, and WD-40 lubricant was sprayed between Teflon films and platens. During low to moderate rate compression tests, a constant engineering strain rate was applied to a final true compressive strain of −0.70.[31]

High strain rate compression testing was conducted on a split Hopkinson pressure bar apparatus designed in cooperation with and built by Physics Applications, Inc. (Dayton, OH). This particular instrument is described in Mulliken and Boyce.[5,6] Specimens for high rate testing were machined to smaller right circular cylinders with diameter 5.05 mm and height 2.7 mm to meet the particular requirements of this test. Specimens were lubricated with a thin layer of petroleum jelly on each surface prior to testing. In the case of high rate testing, samples were tested under true strain rates at yield from 700/s to 3000/s.

Uniaxial tensile tests were also performed on the Zwick mechanical tester. All specimens were tested at a strain rate of 10^{-3}/s until final failure. Extensometers were employed to determine the tensile strains. Pelletized materials were compression-molded into dog-bone-shaped specimens with gauge length of 25.4 mm, thickness of 1.6 mm, and width of 4.2 mm.

3. Results and Analysis

3.1. Miscibility. All PVC/POSS blends with POSS content below 15 wt % were transparent, while the 20 wt % POSS sample is opaque. Miscibility of the PVC/POSS blends was further examined using transmission electron microscopy (TEM).

CDV

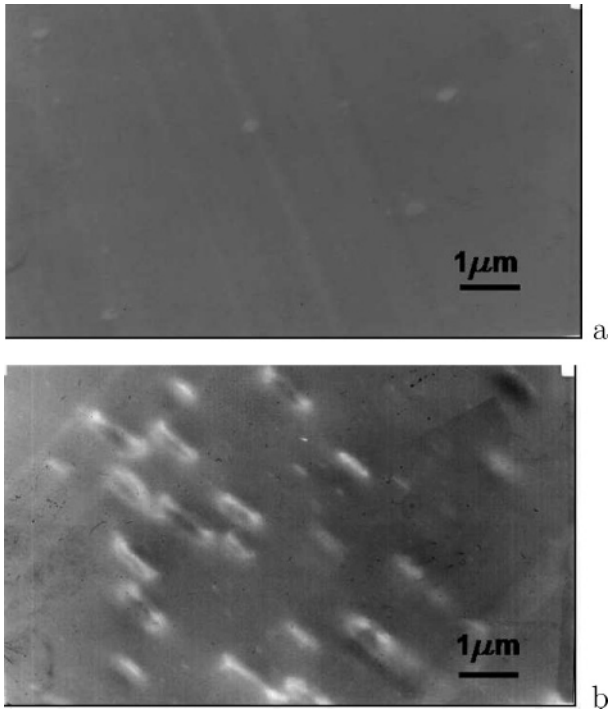

Figure 3. Transmission electron micrographs of the PVC/POSS blends: 15 wt % methacryl-POSS (a) and 20 wt % methacryl-POSS (b).

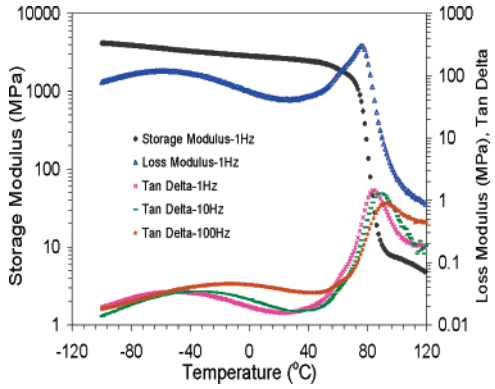

Figure 4. PVC storage modulus, loss modulus, and tan δ curves as a function of temperature at 1 Hz (0.005/s). The tan δ is also shown at 10 and 100 Hz.

Figure 3a shows a micrograph of 15 wt % POSS in PVC, and it appears to be a miscible system. Figure 3b shows a micrograph of 20 wt % POSS in PVC, revealing a second phase of submicron-sized aggregates throughout the sample. The POSS aggregates were squeezed and deformed during microtoming, resulting in the long elliptic morphology. Additional evidence of POSS aggregation in the 20 wt % blend is seen in DMA results as discussed later. All of the PVC/DOP blends in this study are transparent and homogeneous.

3.2. Dynamic Mechanical Analysis. PVC. Storage modulus, loss modulus, and tan δ curves of neat PVC at a converted strain rate of 0.005/s (1 Hz) are shown in Figure 4. As temperature is increased and PVC goes through the β-transition, the storage modulus gradually decreases from 4.2 to 3.0 GPa, and a broad transition peak appears in the loss modulus and tan δ. At the α-transition, the storage modulus drops sharply from 2.5 GPa to 5.0 MPa, and a narrower and more intense peak can be seen in the loss modulus and tan δ. On the basis of the peak values of tan δ at 0.005/s strain rate, PVC has a β-transition temperature of -50 °C and an α-transition temperature of 85 °C.

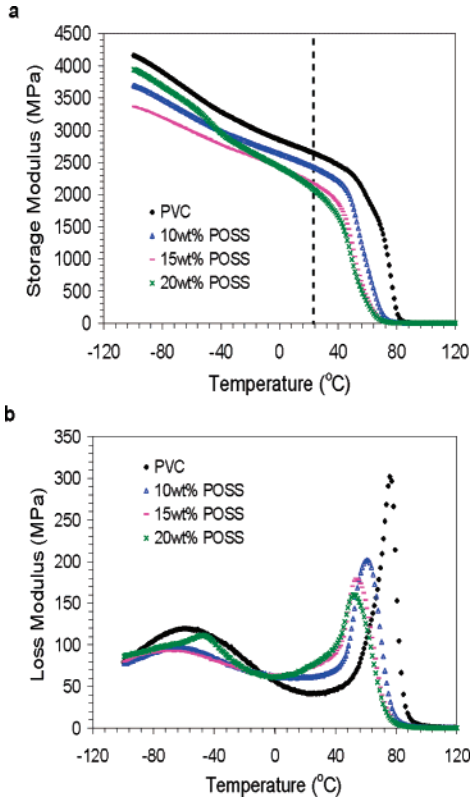

Figure 5. Storage modulus (a) and loss modulus (b) of PVC/POSS blends as a function of temperature at 1 Hz (0.005/s). A vertical dashed line is provided at room temperature for reference purposes.

The locations of the α-transition and the β-transition peaks shift to higher temperatures with increasing strain rate. By testing the material at higher frequencies in the DMA, the strain rate experienced by the sample is increased. Figure 4 shows the shifting of the α-peak and the β-peak of tan δ for PVC. Since the β-transition has a much lower activation energy ($\sim$14.4 kcal/mol) when compared to the α-transition ($\sim$66 kcal/mol) in PVC, the β-transition peak shifts faster than the α-transition. The β-peak shifted from -50 °C at 1 Hz to -11 °C at 100 Hz, whereas the α-peak shifted from 85 °C at 1 Hz to 93 °C at 100 Hz. Wider α- and β-transition peaks are also observed at higher strain rates.

PVC−POSS. Figure 5 shows the storage and loss modulus curves for 10, 15, and 20 wt % methacryl-POSS in PVC. The α-transition temperature decreases monotonically for 10 and 15 wt % blends, suggesting that free volume increases in the PVC upon addition of POSS molecules. Thus, the POSS is acting as a plasticizer. A small inflection in the storage modulus and a bump in loss modulus were observed near -42 °C in the 20 wt % blend. Differential scanning calorimetry measurements (DSC, TA Instruments) give -42 °C as the glass transition temperature of methacryl-POSS itself; thus, the observation of a bump at -42 °C in the DMA is attributed to the aggregated POSS pools in the 20 wt % blend. The maximum amount of this methacryl-POSS that could be incorporated into PVC homogeneously through melt-blending is somewhere between 15 and 20 wt %. Therefore, the α-transition temperature no longer decreases with increasing POSS concentration at concentration greater than 15 wt % POSS.

The β-transition temperature shifts to a lower temperature, and the β-peak lowers and broadens when methacryl-POSS was added. Therefore, the POSS has a plasticizing effect on the β-transition as well as the α-transition due to the liberating effect of free volume on the local motions.

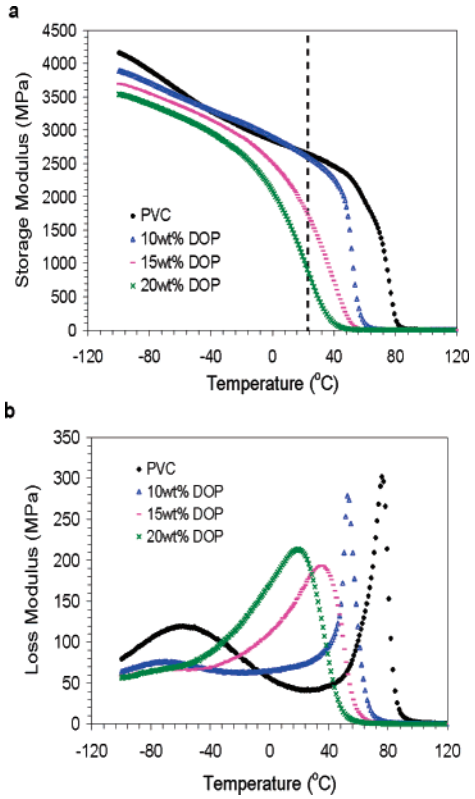

Figure 6. Storage modulus (a) and loss modulus (b) of PVC/DOP blends as a function of temperature at 1 Hz (0.005/s). A vertical dashed line is provided at room temperature for reference purposes.

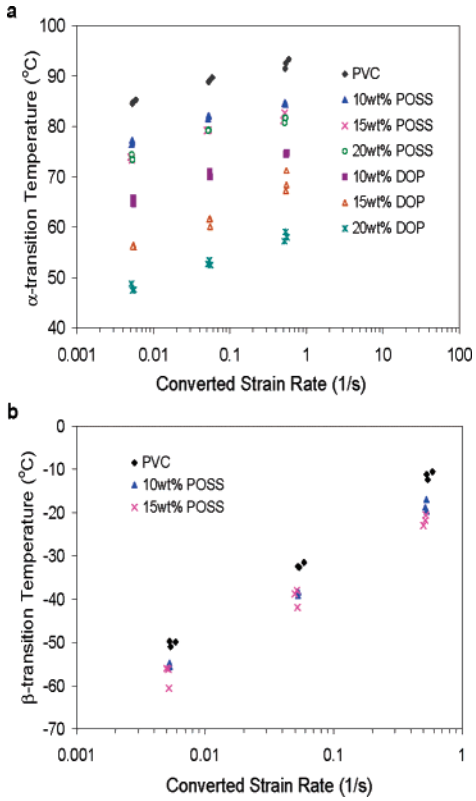

Figure 7. α-transition temperature (a) and *β*-transition temperature (b) of PVC/POSS and PVC/DOP blends as a function of applied strain rate (tan *δ* peak value in DMA).

PVC−DOP. Figure 6 shows the storage and loss modulus curves of 10, 15, and 20 wt % DOP in PVC. The α-transition temperature decreases monotonically with the addition of DOP up to 20 wt %, and the α-transition peak also broadens. In the case of the 20 wt % DOP compound, the storage modulus drop-off begins at approximately −20 °C and reaches fully rubbery behavior at around 40 °C. The *β*-transition is heavily suppressed with increasing DOP content, as evidenced by the dramatic reduction in the magnitude of the *β*-transition loss modulus peak. Only a very small hump was seen near −70 °C in the loss modulus of the 10 wt % blend, and the peak becomes unrecognizable when DOP concentration is at or above 15 wt %. Furthermore, the storage modulus of the 10 wt % DOP blend (Figure 6a) was slightly higher than the pure PVC in the temperature range between the *β*- and α-transitions. Such unexpected mechanical behavior has been observed in slightly plasticized PVC in the glassy state below the glass transition temperature. An increase in modulus, a decrease in creep compliance, and a decrease in impact strength have been documented in PVC containing relatively low concentrations of plasticizers (typically less than 15 wt %),[18−21] and this mechanical behavior is termed "antiplasticization".

The decreasing intensity of the *β*-peak has been observed in many PVC−plasticizer systems since the late 1960s.[18−24] As the plasticizer content increases, the *β*-peak gradually decreases and ultimately vanishes. The suppression of *β*-motions is explained by localized interactions between the plasticizer molecules and the PVC repeat units. Vilics et al.[19] proposed that a strong affiliation is established between the aromatic rings of the plasticizer and the PVC backbones, thereby hindering the local short segmental motions (*β*). Such interaction continues to hinder these local motions even when the temperature exceeds the *β*-transition temperature and therefore results in a higher modulus at temperatures between the *β*- and α-transitions. In the case of PVC/DOP, the interaction that hinders the *β*-motions is the strong hydrogen-bonding between the carbonyl group (⟩C═O) of DOP and the PVC repeat unit (⟩CHCl).[25]

POSS vs DOP. Unlike DOP, the methacryl-POSS does not restrict the *β*-motions in PVC and therefore does not "antiplasticize" the PVC. The methacryl-POSS molecule is larger than the DOP molecule, and its bulky, quasi-spherical structure restricts the molecule from such close affiliation with the PVC backbone. The *β*-motions of the PVC/POSS blends are not hindered as in the case of PVC/DOP. It is seen in Figure 5b that the loss modulus *β*-peak is reduced in the case of PVC/POSS blends, partially due to the decreasing PVC weight fraction and partially due to the POSS plasticizing the local *β*-process.

The α- and *β*-transition temperatures were identified by the α- and *β*-peak values of the tan *δ* curves. The methacryl-POSS is able to reduce both the α- and *β*-transition temperatures in the PVC while the DOP reduces the α-transition temperature but restricts the *β*-motions. Figure 7a summarizes the rate dependency of α-transition of all blends. Incorporating either methacryl-POSS or DOP lowers the α-transition temperature. The α-transition temperature shifts to higher temperatures with increasing strain rate. The α-transition of PVC shifts approximately 3.8 °C per decade increase in strain rate. Table 1 shows that within the DMA testing range the shifting rate of the α-transition temperature in all blends ranges from 3.8 to 5.1 °C per decade increase in strain rate.

The rate dependence of the *β*-transition of PVC/POSS blends is shown in Figure 7b. The *β*-transition temperature is lowered ∼7 °C when 10 or 15 wt % methacryl-POSS is added. The *β*-peak shifting rate of the two blends remains approximately the same as neat PVC. The *β*-peak values in tan *δ* suggests that *β*-transition shifts nearly 17.4 °C per decade increase in strain rate, which indicates that *β*-transition is more sensitive

Table 1. Shifting of α- and *β*-Transition Temperatures (tan *δ* Peak Value in DMA)

	α [°C/decade strain rate]	*β* [°C/decade strain rate]
PVC	3.8	17.4
10 wt % POSS	3.8	17.0
15 wt % POSS	4.0	16.8
20 wt % POSS	3.8	
10 wt % DOP	4.8	
15 wt % DOP	5.0	
20 wt % DOP	5.1	

to strain rate than the α-transition. The *β*-process becomes significant in the mechanical behavior when its rapid shifting with strain rate causes the *β*-transition to move into the experimental window of deformation rate at the testing temperature. PVC/DOP data are not included in Figure 7b since the *β*-motions are suppressed.

3.3. Compression Testing. Rate Dependence of Stress−Strain Behavior. Compression testing was conducted using the Zwick machine and the split Hopkinson bar for low and high strain rate testing, respectively. All specimens were tested to large strains, capturing the elastic, initial yield, and postyield behavior. Deformation was homogeneous in all compression tests; no cracks or other fracture events were observed. Figures 8−10 show the compression stress−strain curves for PVC, 15 wt % POSS, and 20 wt % DOP, respectively, at tested strain rates. The rate-dependent behavior is clearly seen in these figures, where the initial yield stress increases with an increase in strain rate.

Similar glassy polymer stress−strain behavior was observed in compression testing for all blends with the exception of 20 wt % DOP in PVC (Figure 10). DMA revealed the PVC/20 wt % DOP material to have an α-transition at 45 °C at a converted strain rate of 0.005/s based on the tan *δ* curve. Therefore, a

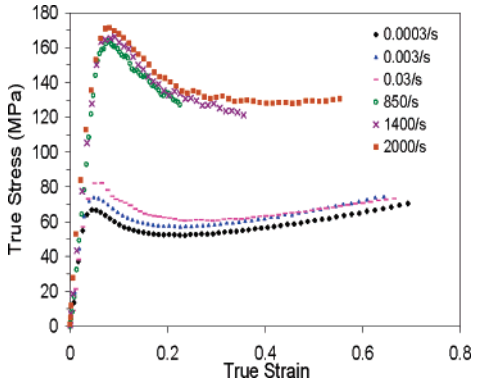

Figure 8. True stress−true strain curves of PVC under different strain rates in compression testing.

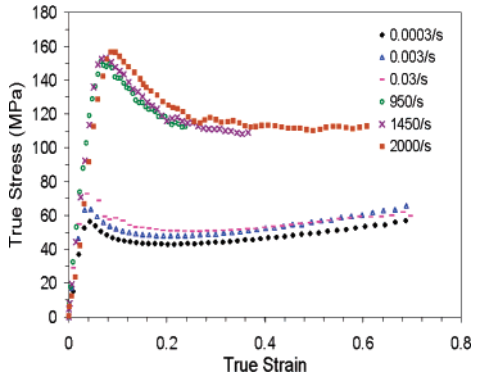

Figure 9. True stress−true strain curves of 15 wt % methacryl-POSS in PVC under different strain rates in compression testing.

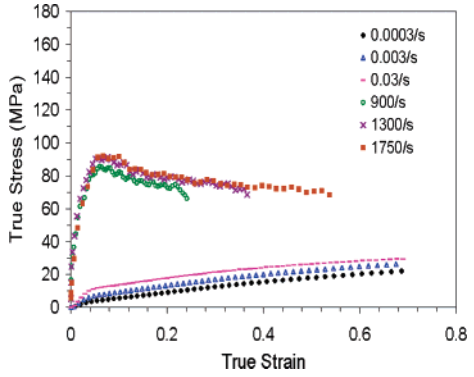

Figure 10. True stress−true strain curves of 20 wt % DOP in PVC under different strain rates in compression testing.

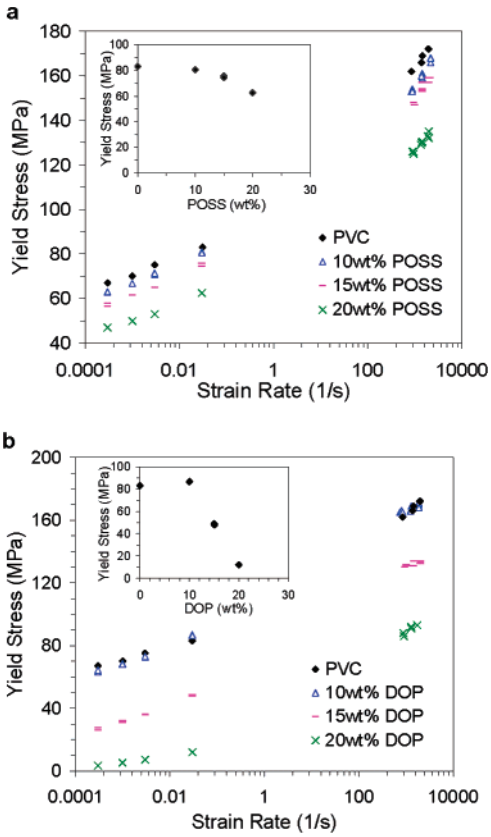

Figure 11. Yield stress as a function of strain rate: PVC/POSS (a) and PVC/DOP (b). Insets show the yield stress as a function of POSS (a) and DOP (b) concentrations at a strain rate of 0.03/s.

rubberlike deformation behavior was expected and found in low rate compression testing (Figure 10). In the case of high rate compression tests, the α-transitions shift to higher temperatures (a linear extrapolation of Figure 7a estimates an α-transition temperature of 76 °C at 2000/s), and glassy polymer deformation behavior was observed again.

Yield stress as a function of strain rate is shown in Figure 11 for all of the materials studied. The neat PVC yield stress increases linearly with the logarithm of strain rate in the low strain rate regime. As strain rate increases into the high rate regime, the yield stress again increases approximately linearly with the logarithm of strain rate. However, the rate dependence is much greater in this high rate regime. At strain rates beyond the transition point, an additional stress is necessary to activate the *β*-process in order to yield the material.

Figure 11a shows the effect of methacryl-POSS on yield stress in PVC. The yield strength decreases with an increase in POSS

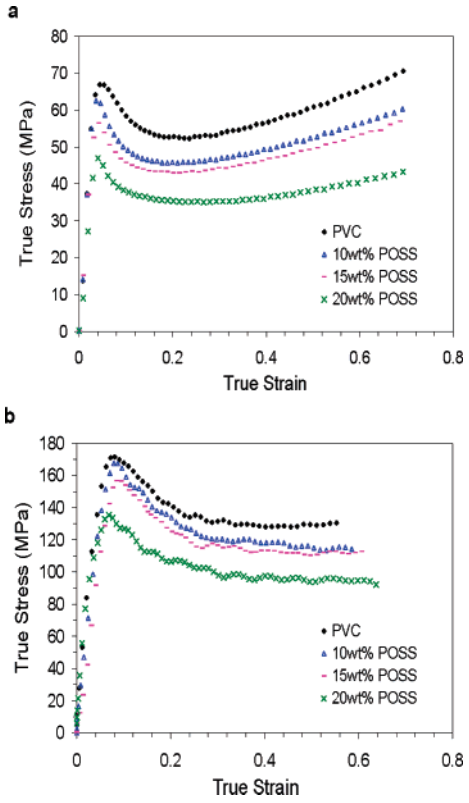

Figure 12. Effect of POSS on true stress−true strain behavior in compression testing: $\dot{\epsilon} = 0.0003$/s (a) and $\dot{\epsilon} \approx 2000$/s (b).

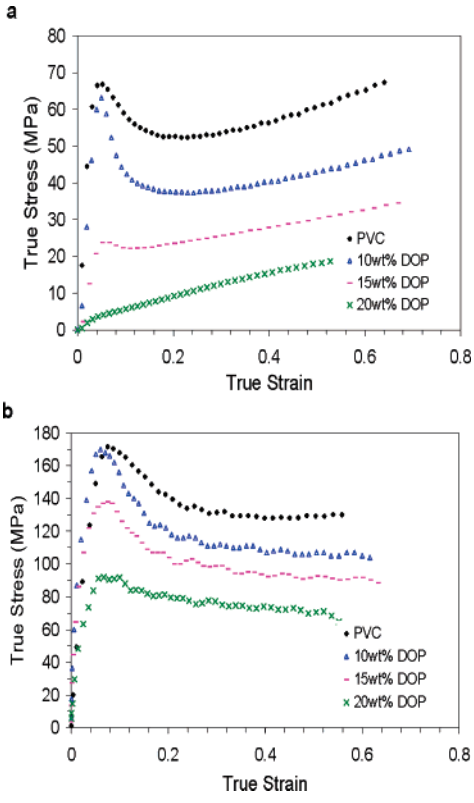

Figure 13. Effect of DOP on true stress−true strain behavior in compression testing: $\dot{\epsilon} = 0.0003$/s (a) and $\dot{\epsilon} \approx 2000$/s (b).

content due to the plasticizing effect of the POSS and the corresponding increased chain mobility. Rate-sensitivity transitions were also observed in the POSS-filled PVC material and again correlates with the rate dependence of the β-transition observed in the DMA. The yield stress as a function of the POSS concentration at 0.03/s strain rate is shown in the inset plot of Figure 11a. The yield stress deceased monotonically with increasing POSS concentration up to 15 wt %. A larger reduction in the yield stress was observed due to the existence of POSS aggregates in the 20 wt % POSS blend.

The rate dependence of yield stress on DOP addition is shown in Figure 11b. The addition of 10 wt % DOP does not appear to alter the yield stress when compared to the neat PVC. This results from the compensating effects of plasticizing the α-motions, acting to decrease the resistance, and antiplasticizing the β-motions, which tends to increase the resistance. Two distinct yield stress rate sensitivities are observed in the 20 wt % DOP-modified materials; however, it is the rate dependence of the α-regime that governs this behavior. The yield strength of the 20 wt % DOP compound is less sensitive to the strain rate in the low rate regime because the material is rubbery; in the high rate regime, this blend behaves like a glassy polymer again; hence, the transition in overall magnitude with the yield stress in the PVC/DOP is a transition from rubbery to leathery to glassy behavior as we go from low rates to very high rates. The yield stress as a function of the DOP concentration at 0.03/s strain rate is shown in the inset plot of Figure 11b. The yield stress of the 10 wt % DOP blend is identical to that of the neat PVC, and at some strain rate it is even higher than the unmodified polymer. Both observations are explained by the absence of a β-transition in the PVC/DOP blends.

Stress−Strain Dependence on Additive Concentration. The effect of POSS and DOP on the entire true stress−true strain behavior of PVC at both low and high strain rates is shown in Figures 12 and 13, respectively. The addition of POSS reduces the yield strength and the flow stress of PVC in both the low strain rate (0.0003/s) and the high strain rate (2000/s) compression tests.

More substantial reductions in the true stress−true strain curves were observed in the case of PVC/DOP blends, and the influence of DOP appears to be different in the low and high strain rates. The yield strength of the 10 wt % DOP blend is nearly identical to the neat PVC in both the low and high strain rates for the reasons discussed earlier; however, the 10 wt % DOP compound exhibits a dramatic postyield strain softening, and hence its flow stress is reduced significantly at all strain rates. Previous publications have shown that a polymer undergoing active plastic deformation at temperature well below T_g is locally in a state that is equivalent to an elevated temperature close to T_g without deformation.[26] This explains the postyield stress−strain behavior of the 10 wt % DOP compound. First we recognize that the 10 wt % DOP blend at room temperature is nearly at T_g. Prior to plastic deformation, the yield stress reflects the combined effect of plasticized α-motions and antiplasticized β-motions, which approximately equals the yield stress of neat PVC. During active plastic deformation, the material is brought to a state that is effectively in the T_g, where the originally restricted β-motions are liberated in addition to the liberation of the main-chain motions. Therefore, the large reduction between the yield stress and the flow stress in the 10 wt % DOP compound is not only due to the conventional strain softening but also due to effectively entering the T_g regime during active plastic deformation. This increased postyyield strain softening during plastic strain of materials very near their T_g has been observed in other polymers (see, e.g., ref 27).

In the low strain rate compression tests, the material behavior changes from glassy to rubbery with increasing DOP content. However, in the high strain rate compression tests, PVC/DOP blends all behave like glassy polymers.

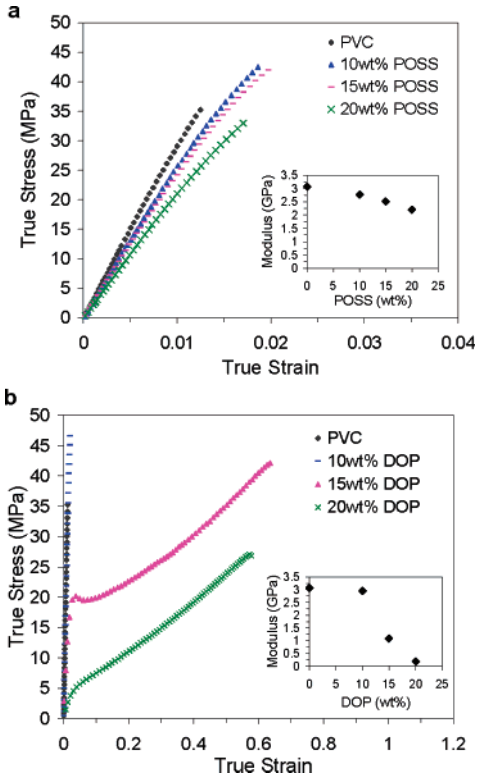

Figure 14. True stress−true strain curves in tensile testing: PVC/POSS (a) and PVC/DOP (b).

3.4. Tensile Testing. Tensile tests were performed to evaluate the tensile toughness and modulus (Figure 14) of the materials. Figure 14a shows the true stress−true strain curves of PVC/POSS compounds in tensile testing. PVC shows brittle behavior, and all specimens fail before reaching the yield point. Although adding methacryl-POSS softens PVC and reduces the modulus, all samples are still brittle and none are able to reach the yield point.

In the case of DOP-filled PVC, specimens are brittle when 10 wt % DOP is added. However, 15 wt % DOP samples exhibit a dramatic increase in tensile toughness, and the strain at break is increased to 65% true strain. 20 wt % DOP samples again are rubbery in the tensile tests and fail at 60% true strain.

3.5. Model vs Experiment. The constitutive model for the rate-dependent elastic−plastic behavior of amorphous polymer proposed by Mulliken and Boyce[5,6] was used to predict the strain rate dependence of the yield stress of the PVC/POSS and PVC/DOP blends in uniaxial compression tests. The rate-dependent yield model follows the essence of the multiple process Ree−Eyring model as utilized by Bauwens-Crowet.[3] Both the primary (α) and secondary (β) processes are considered in the model from low to high strain rates. The total yield stress of the material is the sum of the α-process (eq 2) and the β-process (eq 3)

$$\sigma_{y,\text{total}} = \sigma_{y,\alpha} + \sigma_{y,\beta} \tag{1}$$

$$\sigma_{y,\alpha} = \frac{\sqrt{3}k\theta(s_\alpha + \alpha_{p,\alpha}p)}{\Delta G_\alpha} \sinh^{-1}\left[\frac{\sqrt{3}\dot{\epsilon}}{\dot{\gamma}^p_{o,\alpha}} \exp\left(\frac{\Delta G_\alpha}{k\theta}\right)\right] \tag{2}$$

$$\sigma_{y,\beta} = \frac{\sqrt{3}k\theta\,(s_\beta + \alpha_{p,\beta}p)}{\Delta G_\beta} \sinh^{-1}\left[\frac{\sqrt{3}\dot{\epsilon}}{\dot{\gamma}^p_{o,\beta}} \exp\left(\frac{\Delta G_\beta}{k\theta}\right)\right] \tag{3}$$

where $\sigma_{y,i}$ ($i = \alpha, \beta$) is the yield stress, $\dot{\epsilon}$ is the axial strain rate,

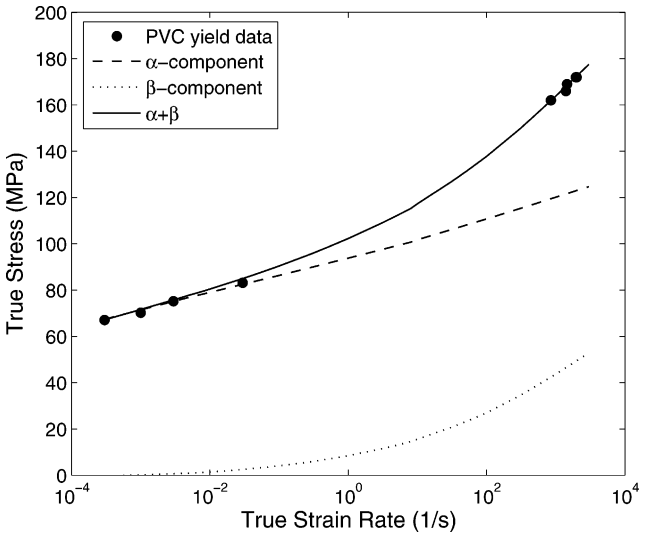

Figure 15. Model prediction of PVC yield stress as a function strain rate.

$\dot{\gamma}^p_{o,i}$ is the preexponential factor, ΔG_i is the activation energy, k is the Boltzmann constant, θ is the absolute temperature, p is the pressure, $\alpha_{p,i}$ is the pressure coefficient, and s_i is an internal variable which captures the material's shear resistance.[28] Following Argon,[29] s_i is given to be

$$s_\alpha(\theta, \dot{\epsilon}) \equiv \frac{0.077\mu_\alpha(\theta, \dot{\epsilon})}{1 - \nu_\alpha} \tag{4}$$

$$s_\beta(\theta, \dot{\epsilon}) \equiv \frac{0.077\mu_\beta(\theta, \dot{\epsilon})}{1 - \nu_\beta} \tag{5}$$

where μ_i is the shear modulus and ν_i is the Poisson ratio. In practice, since the material is considered under high stress at the yield point and the backward progress of the plastic transition is negligible compared to the forward progress, the approximation $\sinh^{-1}(x) \cong \ln(2x)$ is made for both the α-process and the β-process. s_i is both temperature- and rate-dependent, which allows us to capture the change in rate sensitivity of yield when the material transitions from rubbery to leathery to glassy.

Figure 15 shows the model prediction of PVC yield stress in compression as a function of the strain rate compared to the experimental compression data. The α-process and the β-process individual contributions to the yield stress at different strain rates are shown in the figure, and the total model prediction is the sum of the α- and β-components. The model is seen to capture the strong transition in rate sensitivity of the PVC as one transitions from low rates to very high rates (>100/s). Note that the α-contribution alone exhibits a gradual, small change in slope with strain rate, but this does not capture the dramatic difference in rate sensitivity observed at high rates. The models show that as the strain rate is increased, the β-motion requires stress-assisted activation, particularly as the strain rate approaches and exceeds 100/s. The need for stress activation of the β-motions at high rate is responsible for the increased rate sensitivity of yield seen at high rates.

Figure 16 shows the total model predictions as well as the isolated β-contributions plotted together with the compression yield data for the PVC/POSS and the PVC/DOP compounds. Table 2 includes the model parameters of both the α- and β-processes calculated from the experimental data. The α-process activation energy (ΔG_α) is ~4 times that of the β-process (ΔG_β), which is consistent with the values obtained from the

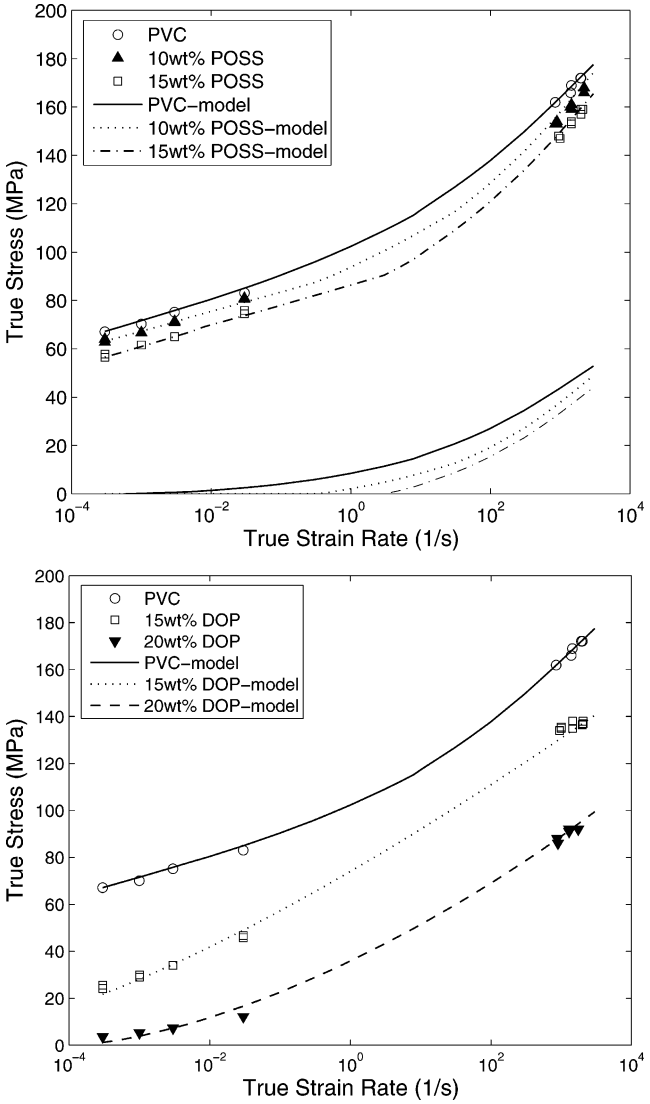

Figure 16. PVC/POSS (a) and PVC/DOP (b) yield strength as a function of strain rate: model prediction and experimental data.

Table 2. Model Parameters for the PVC/POSS and the PVC/DOP

	ΔG_α [J]	ΔG_β [J]	$\dot{\gamma}^p_{0,\alpha}$ [s^{-1}]	$\dot{\gamma}^p_{0,\beta}$ [s^{-1}]
PVC	3.10×10^{-19}	9.19×10^{-20}	9.97×10^{18}	8.21×10^{6}
10 wt % POSS	2.71×10^{-19}	3.81×10^{-20}	1.12×10^{16}	7.55×10^{3}
15 wt % POSS	2.47×10^{-19}	2.54×10^{-20}	1.89×10^{14}	2.97×10^{3}
15 wt % DOP	1.37×10^{-19}		6.92×10^{8}	
20 wt % DOP	1.26×10^{-19}		9.27×10^{9}	

DMA data. The model is seen to capture the transition in rate sensitivity of the yield stress. In the PVC/POSS blends (Figure 16a), the model finds the β-process to require stress-assisted activation at a slightly higher strain rate with increasing POSS content. Such prediction is consistent with the DMA data, in which the β-transition temperature was found to decrease slightly when the methacryl-POSS is added. In the PVC/POSS blends, the β-contribution results in the change in rate sensitivity of yield at high strain rates giving as much as a 40 MPa increase in yield stress over that of the α-contribution alone.

In the 15 and 20 wt % DOP/PVC compounds (Figure 16b), the β-contribution is fully restricted below the glass transition and thus does not manifest itself as a distinct additional contribution at specific temperatures or strain rates. Therefore, yield is modeled as a single lumped activated process. The model shows that the rate sensitivity of yield is fully captured using a single activation approach for the PVC/DOP compounds. In particular, for the 20 wt % DOP blend, the rate sensitivity of yield as one moves from the low to the high strain rate regime is because the material transitions from being in a rubbery regime of response at the low rate to a glassy regime of response at the high rate. Hence, the transition in rate sensitivity of yield is fully predictable as a single lumped stress-activated event for PVC/DOP compounds, in stark contrast to the PVC and PVC/POSS compounds.

4. Conclusions

Methacryl-POSS and DOP were incorporated into PVC through a melt-blending process, and the rate-dependent mechanical behavior of these materials was studied using DMA and large strain compression tests. The PVC/POSS blends are homogeneous and transparent with up to 15 wt % POSS; above 15 wt %, methacryl-POSS forms submicron-sized aggregates in the blend. Within the homogeneous regime, T_g (α-transition) decreases monotonically with increasing POSS content. The β-transition temperature shifts to a lower temperature, and the peak becomes broader with the addition of methacryl-POSS. PVC α- and β-transitions shift to higher temperatures with increasing strain rate, shifting 3.8 and 17.4 °C per decade increase in strain rate for the α- and the β-transitions, respectively. No significant change in the shifting rate of the α-peak or the β-peak was found in the PVC/POSS blends.

In the case of DOP, the same trends in the decreasing and shifting of the α-transition temperature with increasing DOP content were observed, and the α-peak broadens with increasing DOP concentration. However, for the β-transition, the peak vanishes and becomes barely recognizable when the DOP concentration is above 10 wt %. The significant suppression of the β-transition peak is attributed to the molecular interaction between the carbonyl group of DOP and the PVC repeat unit. This interaction attracts the DOP molecules along the PVC main chain and hinders the local β motions, resulting in an antiplasticization of the β-transition when DOP is added. The difference between incorporating methacryl-POSS and DOP into PVC in the β-transition is explained by the differences in molecular size and shape of POSS and DOP. The bulkiness and quasi-spherical shape restrict POSS molecules from approaching the PVC backbone.

Both POSS and DOP plasticize the PVC. The compression yield stress of PVC decreases monotonically with increasing POSS concentration. In the case of PVC/DOP, the antiplasticization of β-motions compensated for the plasticization of α-motions in 10 wt % DOP blend leading to no real change in yield stress when compared to neat PVC. The yield stress decreases beyond 10 wt % DOP added.

A clear rate-sensitivity transition is observed in the compression yield data of pure PVC and PVC/POSS blends between the low rate (<1/s) and the high rate (>500/s) regimes. This transition is attributed to the need for stress-assisted activation of β-motions at high strain rates, which provides a significant increase in the barrier to plastic flow and hence the increased rate-sensitivity of yield. A transition in rate sensitivity is also observed in the DOP blends; this transition is due to the rubbery-to-leathery-to-glassy transition as one goes from the low-to-moderate-to-high strain rates. A constitutive model was used to predict the yield behavior of the PVC compounds. The two-process model captures the stress activation of the α-motions to govern the rate sensitivity at low strain rates; at higher strain rates, the β-motions also require stress activation to enable plastic flow and hence provide the observed increase in rate sensitivity of yield at high rates. In contrast, the β-motions are

suppressed over the entire glassy regime of the material, and the rate-dependent yielding is captured by a single lumped activated process. The apparent increase in rate sensitivity of the PVC/DOP blends is then naturally captured by the model as a result of transitioning through the rubbery-leathery-glassy regimes at different strain rates.

Adding DOP also increases the tensile toughness of PVC. While the modulus decreases from 3000 to 1000 MPa with 15 wt % DOP added, the strain at break increased from 1% to 65% true strain. Unlike DOP, the POSS-filled materials remain brittle in tensile tests.

Acknowledgment. This research was sponsored, in part by the U.S. Army through the Institute for Soldier Nanotechnologies under Contract DAAD-19-02-D-0002 with the U.S. Army Research Office and, in part, by USAFOSR through the DURINT Polymer Nanocomposites, Grant F49620-01-1-0447. We also acknowledge the Chyn Duog Shiah Memorial Fellowship for providing financial support to S. Y. Soong during the academic year 2005−2006. Special thanks to Dr. Edward T. Kopesky for helpful discussions regarding POSS.

References and Notes

(1) Roetling, J. A. *J. Polym.* **1965**, *6*, 311.
(2) Bauwens-Crowet, C. *J. Mater. Sci.* **1973**, *8*, 968.
(3) Bauwens-Crowet, C.; Bauwens, J. C.; Homès, G. *J. Polym. Sci., Part A-2* **1969**, *7*, 735.
(4) Bauwens, J. C. *J. Mater. Sci.* **1972**, *7*, 577.
(5) Mulliken, A. D.; Boyce, M. C. *Int. J. Solids Struct.* **2006**, *43*, 1331.
(6) Mulliken, A. D.; Boyce, M. C. *Proceedings of the 2004 SEM X International Congress and Exposition on Experimental and Applied Mechanics*, paper #197, 2004.
(7) Böhning, M.; Goering, H.; Hao, N.; Mach, R.; Schönhals, A. *Polym. Adv. Technol.* **2005**, *16*, 262.
(8) Böhning, M.; Goering, H.; Fritz, A.; Brzezinka, K.; Turky, G.; Schönhals, A.; Schartel, B. *Macromolecules* **2005**, *38*, 2764.
(9) Kuila, B. K.; Nandi, A. K. *Macromolecules* **2004**, *37*, 8577.
(10) Xu, H.; Kuo, S.; Lee, J.; Chang, F. *Macromolecules* **2002**, *35*, 8788.
(11) Mather, P. T.; Jeon, H. G.; Romo-Uribe, A. *Macromolecules* **1999**, *32*, 1194.
(12) Zheng, L.; Farris, R. J.; Coughlin, E. B. *Macromolecules* **2001**, *34*, 8034.
(13) Phillips, S. H.; Haddad, T. S.; Tomczak, S. J. *Curr. Opin. Solid State Mater. Sci.* **2004**, *8*, 21.
(14) Kopesky, E. T.; Haddad, T. S.; Cohen, R. E.; McKinley, G. H. *Macromolecules* **2004**, *37*, 8992.
(15) Capaldi, F. M.; Rutledge, G. C.; Boyce, M. C. *Macromolecules* **2005**, *38*, 6700.
(16) Mulliken, A. D.; Boyce, M. C. *J. Eng. Mater. Technol.*, submitted for publication.
(17) Kopesky, E. T.; McKinley, G. H.; Cohen, R. E. *Polymer* **2005**, *46*, 4743.
(18) Kinjo, N.; Nakagawa, T. *Polym. J.* **1973**, *4*, 143.
(19) Vilics, T.; Schneider, H. A.; Manoviciu, V.; Manoviciu, I. *J. Therm. Anal.* **1996**, *47*, 1141.
(20) Pezzin, G.; Ajroldi, G.; Garbuglio, C. *J. Appl. Polym. Sci.* **1967**, *2*, 2553.
(21) Sundgren, N.; Bergman, G.; Shur, Y. *J. Appl. Polym. Sci.* **1978**, *22*, 1255.
(22) Dubault, A.; Bokobza, L.; Gandin, E.; Halary, J. L. *Polym. Int.* **2003**, *52*, 1108.
(23) Elícegui, A.; del Val, J. J.; Millán, J. L.; Mijangos, C. *J. Non-Cryst. Solids* **1998**, *235*, 623.
(24) Elícegui, A.; del Val, J. J.; Bellenger, V.; Verdu, J. *Polymer* **1997**, *38*, 1647.
(25) Garnaik, B.; Sivaram, S. *Macromolecules* **1996**, *29*, 185.
(26) Zhou, Q.-Y.; Argon, A. S.; Cohen, R. E. *Polymer* **2000**, *42*, 613.
(27) Dupaix, R. B.; Boyce, M. C. *Polymer* **2005**, *46*, 4827.
(28) Boyce, M. C.; Parks, D.; Argon, A. S. *Mech. Mater.* **1988**, *7*, 15.
(29) Argon, A. S. *Philos. Mag.* **1973**, *28*, 839.
(30) The frequency ω of each test is converted to a strain rate by examining one-quarter of the sinusoidal loading cycle. The time duration of this quarter cycle is known from the test frequency, and the maximum strain amplitude achieved during this time is measured during the test. It is assumed that the increase in strain over this time is approximately linear, and an average strain rate can be calculated: $\dot{\epsilon}$ = strain/time $= 4\epsilon_0\omega$, where ϵ_0 is the maximum strain amplitude achieved at one-quarter of the loading cycle.
(31) Where true strain is taken to be $\ln(h/h_0)$ with h being current sample height and h_0 being initial sample height. Engineering strain is taken to be $\Delta h/h_0$.

MA052736S